

5.2. Palmer Station (5/13/99 – 3/9/00)

The 1999-2000 season at Palmer Station is defined as the time between the site visits 05/03/99 - 05/25/99 and 3/9/00 – 3/19/00. The season opening and closing calibrations were performed on 5/11/99 and 3/10/00, respectively. Volume 9 solar data comprises the period 5/13/99 – 3/9/00. Between 5/14/99 and 5/25/99, the on-site TUVR and PSP were compared with traveling instruments. No PSP and TUVR data of this time are published; spectral UV measurements are not affected. The system functioned normally during the Volume 9 period, with the following exceptions:

- A new PMT cooler power supply was installed during the 1999 site visit. Compared to its predecessor, the temperature regulation is more accurate, which is accomplished via a switching PID controller. The switching unfortunately introduced excess noise in the PMT current due to a ground loop. For solar elevations higher than 20° and wavelengths below 345 nm, the detection limit¹ is approximately 0.003 $\mu\text{W cm}^{-2} \text{nm}^{-1}$, which is by a factor of three higher than the typical value 0.001 $\mu\text{W cm}^{-2} \text{nm}^{-1}$. The detection limit for solar elevations below 20° is approximately 0.0007 $\mu\text{W cm}^{-2} \text{nm}^{-1}$. This is only slightly above the normal value of 0.0005 $\mu\text{W cm}^{-2} \text{nm}^{-1}$. The effect of the problem on published dose-rates is almost negligible because signal levels in the relevant spectral regions are well above the increased noise level, except when solar elevation is below 2°. The noise has been reduced during the site visit in 2000 by improving the ground connection of the PMT. A change of the temperature set point implemented in January 2001 finally brought noise levels back to normal.
- The monochromator position indicator became sticky between 2/13/00 and 2/24/00 before it completely jammed on 2/25/00, preventing the monochromator from turning. The indicator was removed on 2/25/00, which solved the problem. In the affected period, wavelength uncertainty is increased, as explained below.
- The system responsivity changed abruptly by approximately 10% between 7/22/99 and 7/23/99 without obvious reasons. Solar data are not affected since the instrument's calibration was adjusted accordingly. Except of this "jump," system responsivity was stable to within $\pm 3\%$.
- There were communication problems between the instrument's High Resolution A/D converter (HRAD) and the computer at the beginning of the season. After rewiring both units on 6/7/99, the problem disappeared. The HRAD is only used to digitize auxiliary sensors, including PSP and TUVR. Incorrect values were excluded from the published dataset. Spectral irradiance data were digitized with a second A/D converter and were not affected.

About 98% of the scheduled data scans are part of the published dataset; less than 1.5% of all scans were lost because of technical problems.

5.2.1. Irradiance Calibration

The site irradiance standards for the 1999-2000 Palmer season were the lamps 200W007, M-765, and M-700. Lamp M-874 was used as the traveling standard. It was calibrated by Optronic Laboratories in September 1998. Lamp 200W007 has an irradiance calibration from Optronic Laboratories from November 1996. Lamp M-765 has an Optronic Laboratories calibration from 1992 and has been in use at Palmer Station since 1992. Comparisons with M-874 and 200W007 indicate that lamp M-765 has drifted by about

¹ Detection limit is defined as the standard deviation of the measured spectral irradiance at 285 nm. At this wavelength, all solar radiation is filtered out by the Earth's ozone layer. The measured value at 285 nm therefore reflects the magnitude of instrument noise, which causes the detection limit.

1-2% over the years. In order to improve the accuracy of the data, lamp M-765 was recalibrated with M-874 using data from the Volume 9 opening calibrations. Lamp M-700 does not have a calibration from a standards laboratory. For use in the 1999-2000 season, the lamp was calibrated in a similar fashion as lamp M-765; the irradiance calibration was transferred from the traveling standard M-874 using absolute scans of both lamps from days 5/11/99 and 5/12/99.

Figure 5.2.1 shows the Volume 9 season opening calibrations performed on 5/11/99 and 5/12/99. All lamps agree on the $\pm 1\%$ level. The good agreement of lamps M-700 and M-765 with M-874 can be expected since the scans depicted in Figure 5.2.1 are the same that were used to establish calibrations for M-700 and M-765. The validity of these calibration is confirmed with the good agreement to lamp 200W007, which has an independent calibration.

Figure 5.2.2 shows the Volume 9 season closing calibrations performed on 3/9/00 and 3/10/00. The agreement of lamps M-700 and M-765 with M-874 is similar as during the season opening scans, suggesting that none of the lamps has drifted. The values for the standard 200W007 also agree in the visible but are approximately 1.5% higher in the UV. The agreement of all lamps, including 200W007 is well within the typical uncertainties of irradiance standards calibrations, giving confidence in the solar data of the Palmer instrument of the 1999-2000 season.

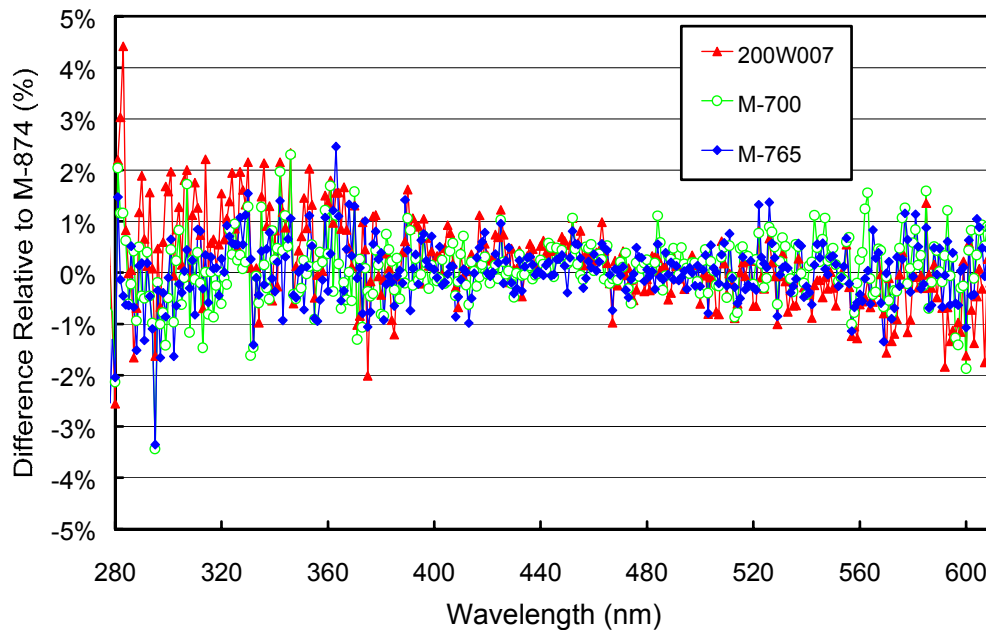


Figure 5.2.1. Comparison of Palmer lamps 200W007, M-700, and M-765 with the BSI traveling standard M-874 at the beginning of the season (days 5/11/99 and 5/12/99).

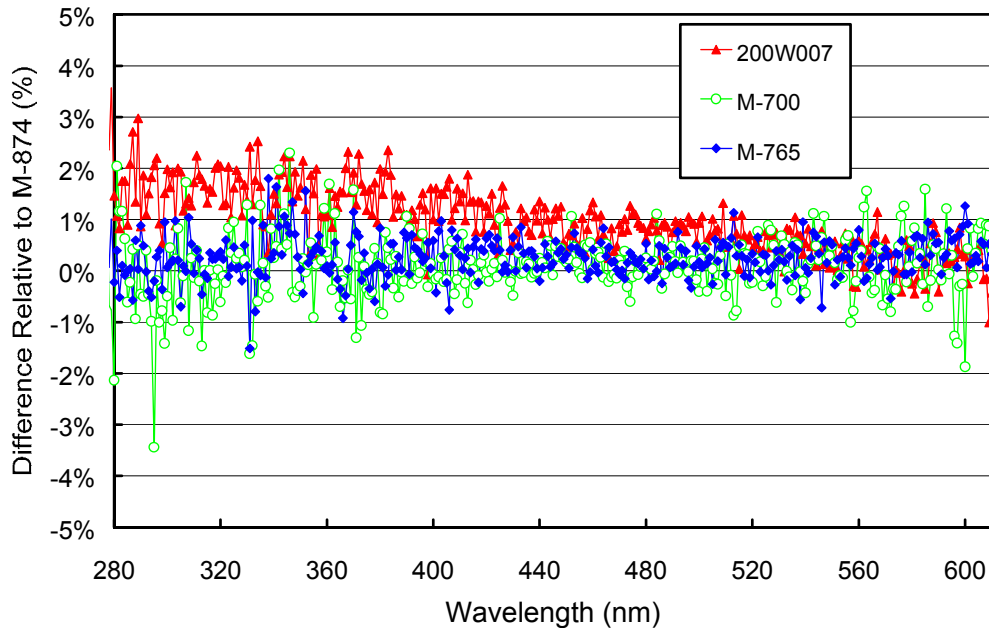


Figure 5.2.2. Comparison of Palmer lamps 200W007, M-700, and M-765 with the BSI traveling standard M-874 at the end of the season (days 3/9/00 and 3/10/00).

5.2.2. Instrument Stability

The stability of the spectroradiometer over time is primarily monitored with bi-weekly calibrations utilizing the site irradiance standards and daily response scans of the internal irradiance reference. The stability of the internal lamp itself is monitored with the TSI sensor, which is independent from possible monochromator and PMT drifts. By logging the PMT currents at several wavelengths during response scans, changes in the instrument responsivity can be detected.

Figure 5.2.3 shows the changes in TSI readings and PMT currents at 300 and 400 nm, derived from the daily response scans of the Palmer 1999-2000 season. The TSI measurements indicate that the internal lamp was very stable during the whole season. The PMT-currents were stable to within $\pm 2\%$ until 7/22/99 and then abruptly decreased by 10-12%. The reason for this change in responsivity could not be identified. Solar data are not affected since the calibration was changed accordingly. After this “jump,” system responsivity increased gradually during the next three months by 2% before it dropped again by 6% during the last four months of the season. Although the internal lamp was stable, calibrations with the 200-Watt site standards suggested that the season has to be split in four periods—denoted Periods 1 – 4—in order to adjust for changes in the through-the-collector responsivity of the instrument.

To establish a calibration in a given period, irradiance spectra for the internal lamp were calculated from all absolute scans in that period. The irradiance spectrum finally assigned to the lamp is the average of these individual spectra (see Section 4.2.1.2 for details). In addition, the standard deviation of these spectra was calculated. Figure 5.2.4 shows the ratio of the standard deviation and average spectra, calculated for each of the four periods. This ratio is useful for estimating the variability of the calibrations in each period. Figure 5.2.4 shows that the standard deviation is usually less than 1% of the average for all periods in the UV-A and visible, and increases slightly towards shorter wavelengths. Thus the calibrations in all periods are consistent to the $\pm 1\%$ ($\pm 1\sigma$) level.

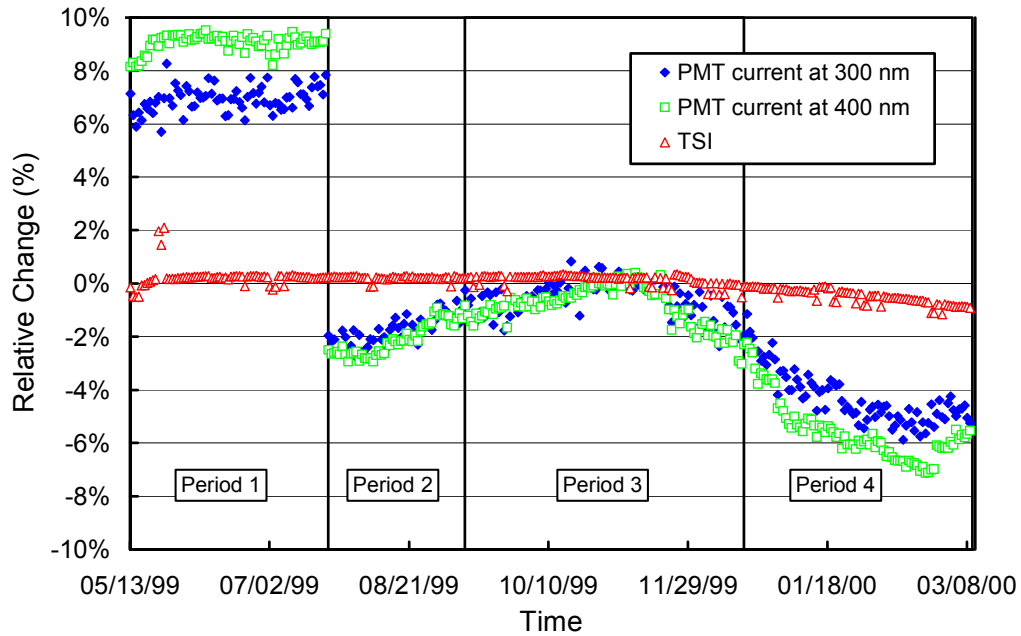


Figure 5.2.3. Time-series of PMT current at 300 and 400 nm, and TSI signal during measurements of the response lamp during the Palmer 1999-2000 season. The data is normalized to the average of all periods.

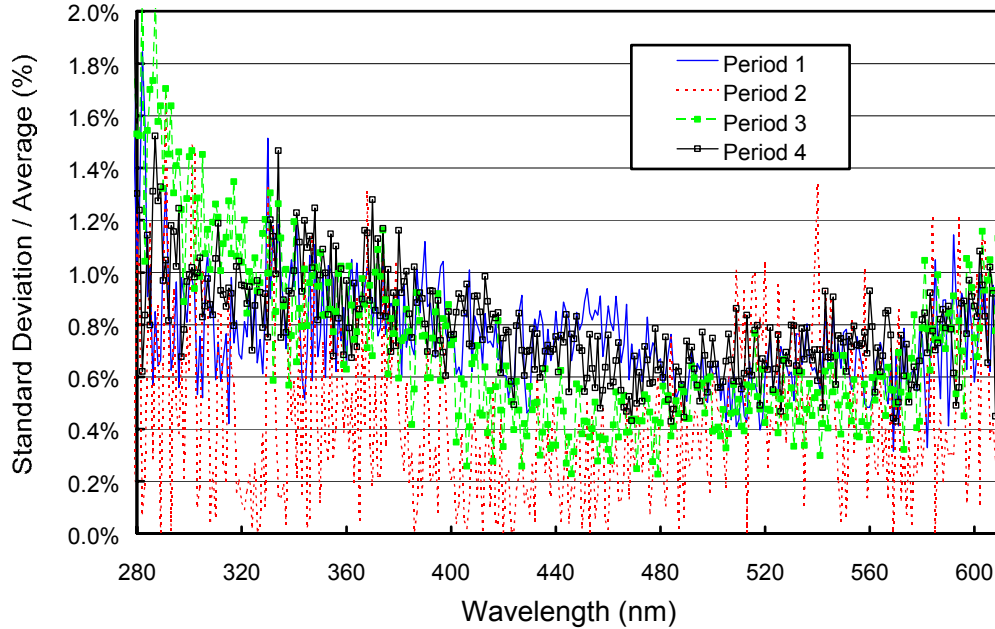


Figure 5.2.4. Ratio of standard deviation and average calculated from the absolute calibration scans of Periods 1 through 4.

Figure 5.2.5 shows the ratio of the irradiance assigned to the internal lamp in Period 1, 3, and 4, referenced to Period 2. The unexplained change in PMT current between Period 1 and 2 manifests itself also in Figure 5.2.5; the ratio Period 1 / Period 2 ranges between 1.07 and 1.13. The changes between Period 2 and 3, and 3 and 4 are less than 2%, respectively.

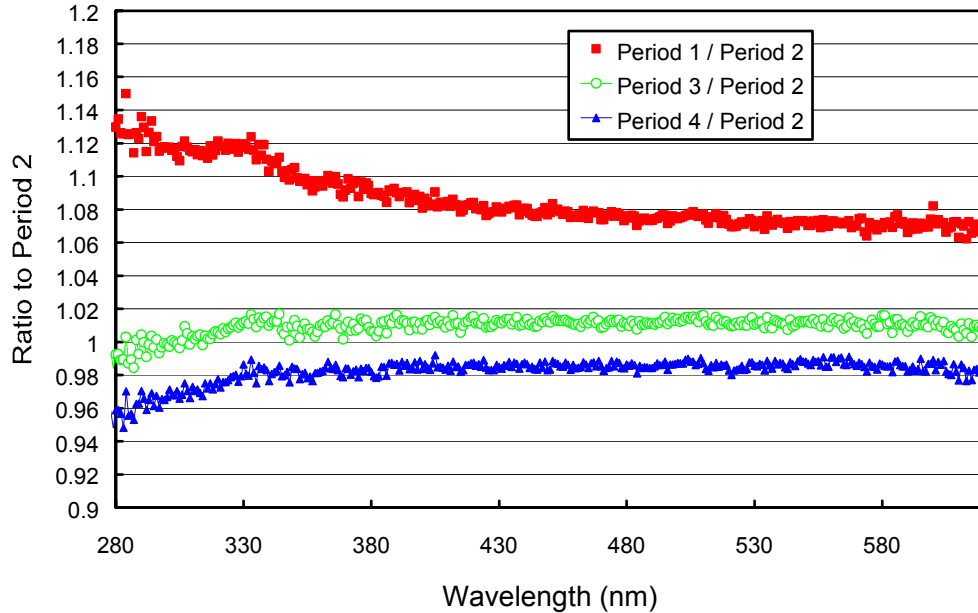


Figure 5.2.5. Ratios of irradiance assigned to the internal reference lamp.

5.2.3. Wavelength Calibration

Wavelength stability of the system was monitored with the internal mercury lamp. Information from the daily wavelength scans was used to homogenize the data set by correcting day-to-day fluctuations in the wavelength offset. After this step, there may still be a deviation from the correct wavelength scale, but this bias should ideally be the same for all days. Figure 5.2.6 shows the differences in the wavelength offset of the 296.73 nm mercury line between two consecutive wavelength scans. In total, 300 scans were evaluated. For 88% of the days, the change in offset was smaller than ± 0.025 nm; for 99% of the days the shift was smaller than ± 0.055 nm. The offset-difference was larger than ± 0.1 nm for only two scans on 2/23/99 and 2/25/99, the period when the dial jammed. The affected period was excluded from the published dataset.

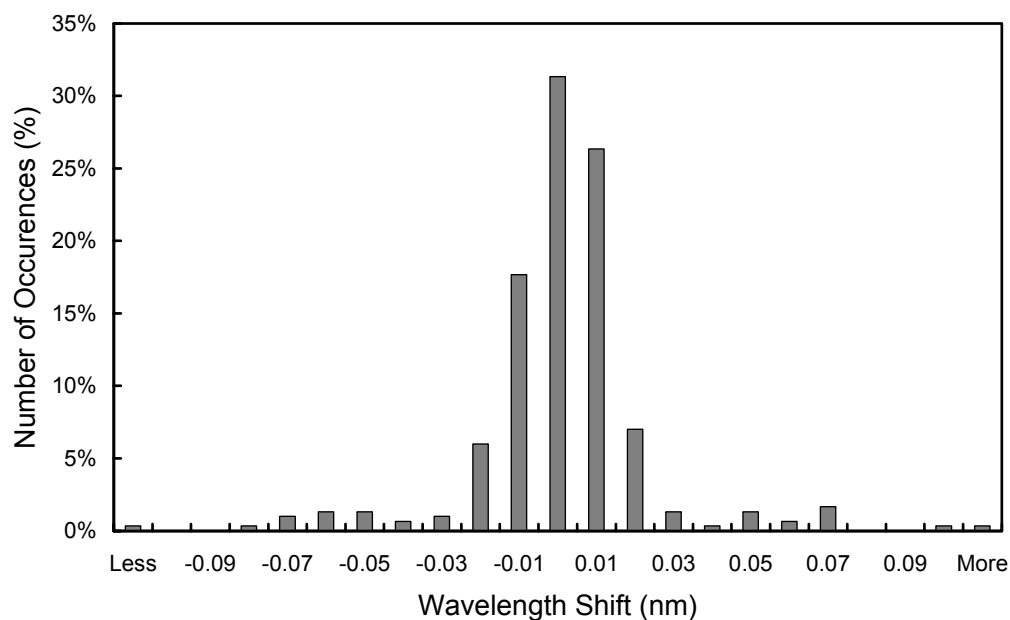


Figure 5.2.6. Differences in the measured position of the 296.73 nm mercury line between consecutive wavelength scans. The x-labels give the center wavelength shift for each column. Thus the 0-nm histogram column covers the range -0.005 to $+0.005$ nm. “Less” means shifts smaller than -0.105 nm; “more” means shifts larger than 0.105 nm.

After the data was corrected for day-to-day wavelength fluctuations, the wavelength-dependent bias between this homogenized data set and the correct wavelength scale was determined with the Fraunhofer-correlation method, as described in Section 4. It appeared that not only the instrument sensitivity changed between Periods 1 and 2, but also the wavelength mapping of the monochromator. Different correction functions for the monochromator non-linearity were therefore established for Period 1 and Periods 2-4. The thick lines in Figure 5.2.7 shows these functions, which are very similar. In order to demonstrate the difference between the result of the Fraunhofer-correlation method and the method that was historically applied (see Section 4.2.2.1), Figure 5.2.7 also includes a correction function that was calculated with the “old” method, i.e., the function is based on internal wavelength scans only.

After the data was wavelength corrected using the shift-function described above, the wavelength accuracy was tested again with the Fraunhofer method. The results are shown in Figure 5.2.8 for four UV wavelengths. The residual shifts are generally smaller than ± 0.1 nm. There is more scatter at 310 nm during the austral winter because of the small solar irradiance levels that prevail during this part of the year. Between 2/13/00 and 2/23/00 residual shifts are slightly larger than ± 0.1 nm. This is caused by jamming of the monochromator position indicator, which was replaced on 2/25/00. The affected period was more closely examined by checking all data scans of each day rather than noon-time measurements only. Figure 5.2.9 shows the wavelengths shifts in the final data between 2/18/00 and 2/28/00. There is significantly more scatter in the shifts until 2/25/00 before the indicator was replaced and wavelength uncertainties went back to normal.

Figure 5.2.7 shows a distinct peak in the monochromator correction function at 380 nm. At this wavelength, the Fraunhofer-based correction function also deviates by more than 0.2 nm from the correction function that is based on internal wavelength scans only. In order to verify whether the peak at 380 nm is real, the wavelength accuracy of the corrected data was additionally checked with the method by Mayer (1997), which is described in Section 4.2.2.2 d. Figure 5.2.10 shows that the residual shifts found with the method by Mayer (1997) agrees to within the error bars with the shift determined with the method by Slaper et al. (1995), which is also used to calculate the correction function. There is no significant difference in the residual shifts at 380 and 390 nm, suggesting that the peak in the correction function at 380 nm is real.

However, further analysis showed that the feature in the correction function between 410 and 440 nm may partly be due to a poor correlation of the correction algorithm in this spectral region. The correction in this region has therefore an additional uncertainty of about ± 0.1 nm.

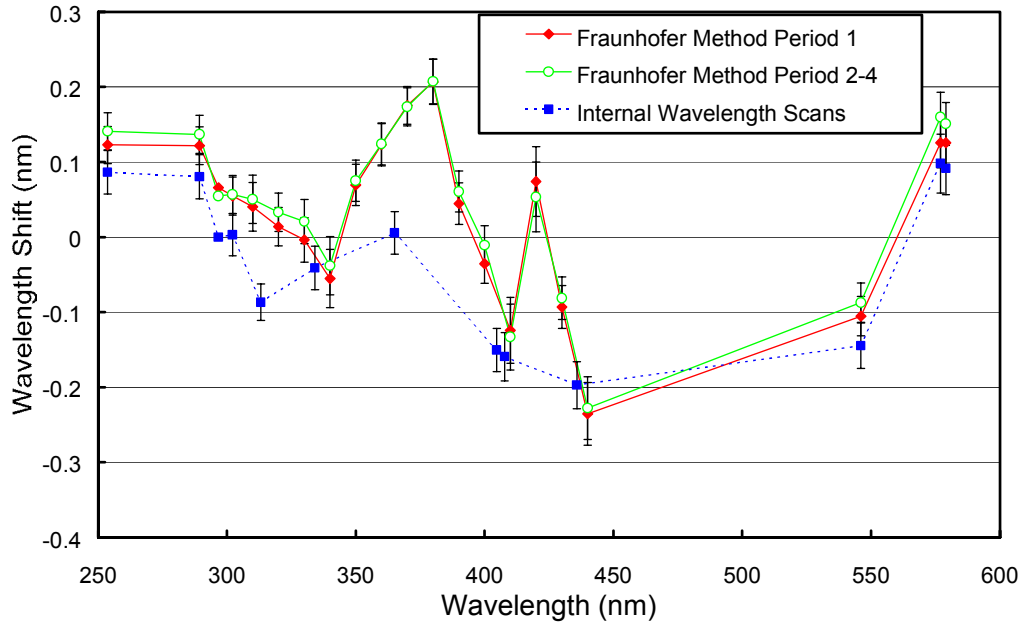


Figure 5.2.7. Monochromator non-linearity for the Palmer 1999-2000 season. Thick line with diamonds: Correction function calculated with the Fraunhofer-correlation method, and applied to correct the Palmer Volume 8 data in Period 1. Thick line with open circles: Fraunhofer correction function applied in Periods 2-4. Thin broken line: Correction function calculated with the method that was historically applied. The error bars show the 1σ standard deviation of the wavelength shifts.

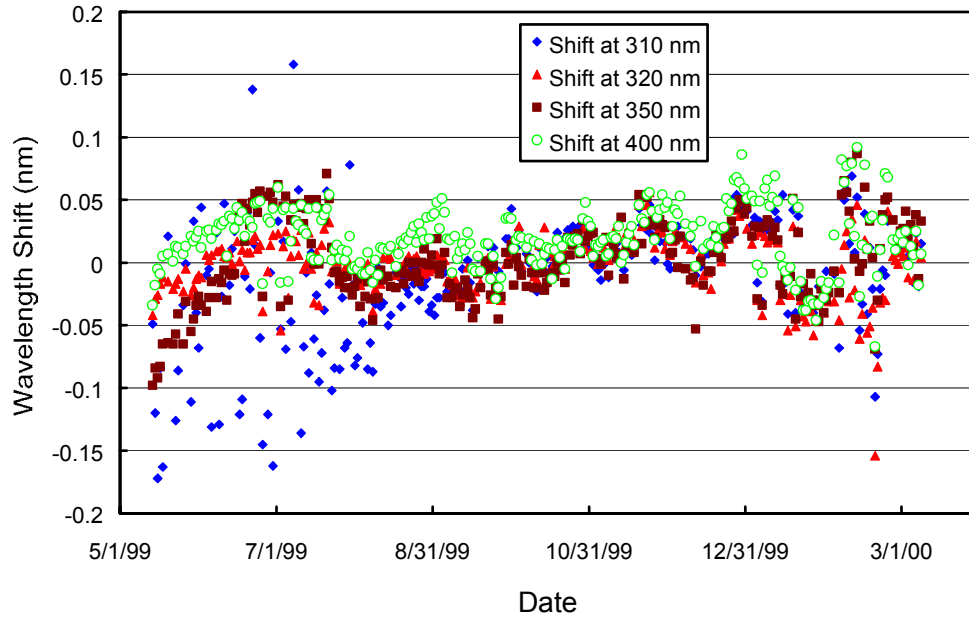


Figure 5.2.8. Wavelength accuracy check of the final data at four wavelengths by means of Fraunhofer correlation. The noontime measurement has been evaluated for each day of the season.

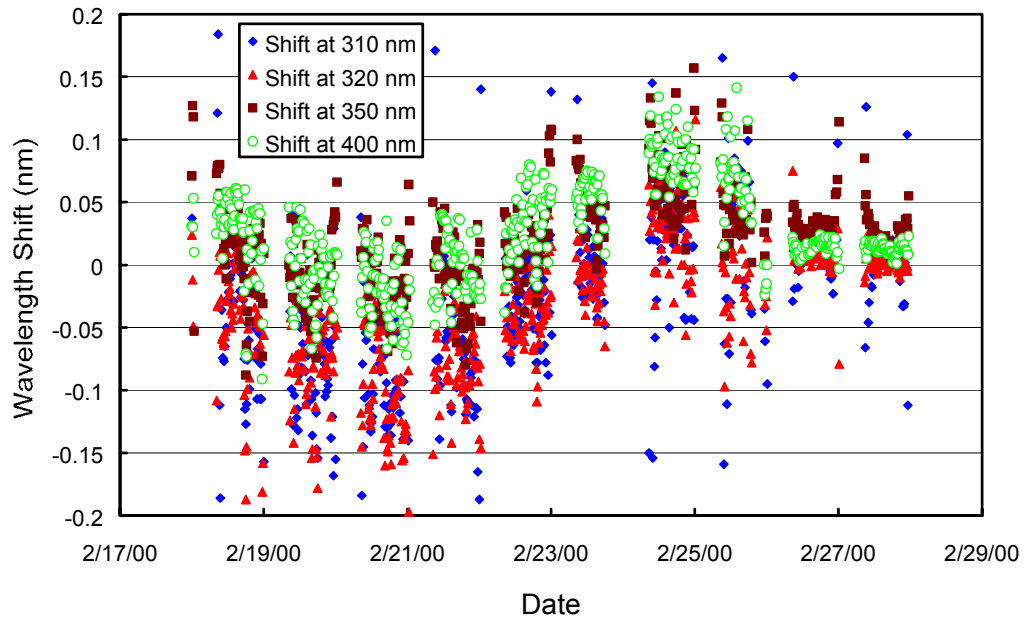


Figure 5.2.9. Wavelength accuracy check of the final data at four wavelengths by means of Fraunhofer correlation between 2/18/00 and 2/28/00. All data scans from the period have been evaluated.

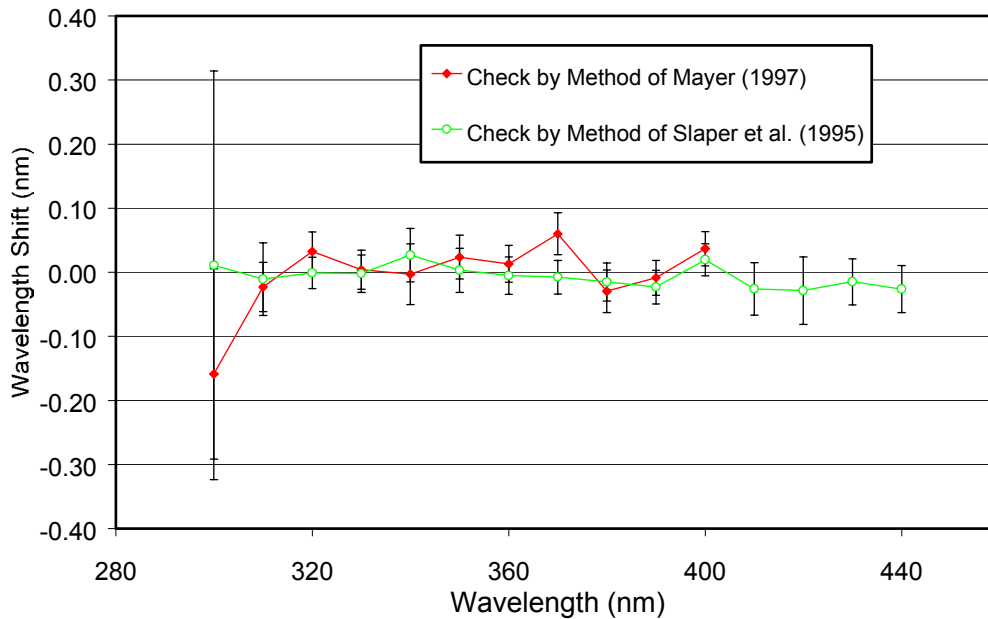


Figure 5.2.10. Average wavelength shift of the corrected data determined with two independent methods. Shifts were averaged over time using data from the whole season. Error bars denote the standard deviation of the shifts.

Although data from the external mercury scans do not have a direct influence on the data products, they are an important part of instrument characterization. Figure 5.2.11 illustrates the difference between internal and external mercury scans collected during both site visits. The wavelength scale of the figure is the same as applied during solar measurements. External scans have a bandwidth of about 0.95 nm FWHM, whereas the bandwidth of the internal scan is only 0.72 nm. Season opening (May 1999) and season closing (March 2000) scans appear to be shifted by approximately 0.05. This is within the range of residual wavelength shifts after wavelength correction (see also Figure 5.2.8). Internal scans of both periods are shifted by about 0.14 nm to shorter wavelength with respect to their external counterparts. Since external scans have the same light path as solar measurements, they more realistically represent the monochromator bandpass relevant for solar scans.

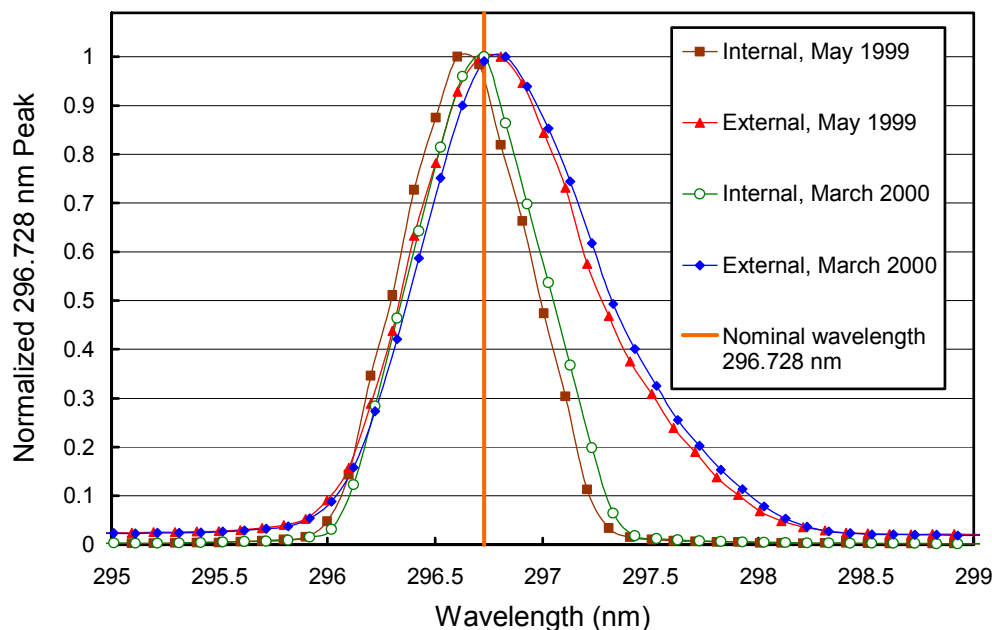


Figure 5.2.11. The 296.73 mercury line as registered by the PMT from external and internal sources. The wavelength scale is the same as applied for solar measurements.

5.2.4. Missing Data

A total of 16225 scans with solar zenith angles smaller than 92° were scheduled to be measured in the Palmer Volume 9 season. Of these scans, 15955 (98.3%) were found to be of good quality and are therefore part of the published dataset. Of the missing scans, 16, 30, and 63 were superseded by absolute, wavelength, and response scans, respectively. Since Palmer Station has almost 24 hours of sunlight per day in December, a loss of data scans cannot be avoided. Approximately 70 scans were lost due to a software problem on 11/18/99. A loose contact of a data cable connecting the High Resolution A/D converter (HRAD) with the computer caused a loss of 32 scans on 5/13/99 and 5/24/99. Thirty additional scans were not recorded because of power outages, surveying activities and unknown reasons. As mentioned in Section 5.2.2, the instrument's sensitivity changed abruptly by 10-12% on 7/22/99. Since the exact time of this change could not be determined, 26 data scans from 7/22/99 were excluded from the data set. A total of 16556 scans are listed in the published databases, including 601 scans with solar zenith angles between 92° and 95° .